Electronic Supplementary Material (ESI) for Physical Chemistry Chemical Physics.

Supplementary information for

Mirror symmetry breaking by mixing of equimolar amounts of two gyroid phase-forming achiral molecules

Shoichi Kutsumizu,*[a] Suguru Miisako,[a] Yohei Miwa,[a] Makoto Kitagawa,[a] Yasuhisa Yamamura[b] and Kazuya Saito[b]

[a]*Department of Chemistry and Biomolecular Science, Faculty of Engineering, Gifu University, 1-1 Yanagido, Gifu 501-1193, Japan.*
[b]*Department of Chemistry, Faculty of Pure and Applied Sciences, University of Tsukuba, Tsukuba, Ibaraki 305-8571, Japan.*

Contents

1. Materials

1.1 Synthesis of the compounds used

1.1.1 1,2-Bis(*n*-alkoxybenzoyl)hydrazine (BABH-*n* with *n* = 8, 10, 14, 18 and 20)

BABH-8, -10, -14, -18, and 20 were prepared basically using the same chemical route developed by Schubert et al.[S1] but with a modified procedure described in our previous paper.[S2] The phase behaviors are also given in Ref [S2].

1.1.2 1-(4′-*n*-decyloxybenzoyl)-2-(4′-*n*-octadecyloxybenzoyl)hydrazine (BABH-10-18)

(a) 4′-*n*-decyloxybenzoic acid (ABA-10)

1-Bromodecane (23.43 g, 106 mmol), ethyl 4-hydroxybenzoate (9.41 g, 57 mmol), and K_2CO_3 (15.97 g, 116 mmol) were dissolved in acetone and refluxed for 24 h. After filtration, the solvent was removed under vacuum. The residue obtained was dissolved in ethanol (120 mL), to which an aqueous solution (40 mL) of NaOH (4.53 g, 113 mmol) was added. The solution was further stirred for 20 h. After cooling to room temperature, the solution was filtered to obtain a white solid. The crude product was dissolved in a mixture of water and ethanol and heated, to which was added 1 N aqueous HCl (35 mL). A white solid precipitated was collected by filtration, recrystallized from a mixture of hexane and a small volume of ethanol, dried under vacuum, to afford 13.68 g (49.1 mmol, 86.8 %) of **ABA-10**.

^{1}H NMR (400 MHz, $CDCl_3$, r.t.): δ 0.88 (t, J = 6.8 Hz, 3H), 1.27-1.50 (m, 14H), 1.82 (quin, J = 7.0 Hz, 2H), 4.02 (t, J = 6.6 Hz, 2H), 6.93 (d, J = 9.0 Hz, 2H), 8.05 (d, J = 8.8 Hz, 2H).

(b) 4′-*n*-octadecyloxybenzoic acid (ABA-18)

1-Bromooctadecane (8.38 g, 25.1 mmol), ethyl 4-hydroxybenzoate (2.78 g, 16.7 mmol), and K_2CO_3 (4.79 g, 35.7 mmol) were dissolved in acetone (200 mL) and refluxed for 32 h. After that, almost the same precedure as described for **ABA-10** was used and the crude product was recrystallized from THF.

(c) 4′-*n*-octadecyloxybenzhydrazide (ABH-18)

A portion of the **ABA-18** obtained above (5.49 g, 13 mmol) and an excess amount of hydrazine monohydrate (22.27 g, 445 mmol) were dissolved in 2-propanol (150 mL) and refluxed for 48 h. After cooling to room temperature, the slurry product was collected and dried in a reduced pressure in a desiccator. The obtained solid was recrystallized from $CHCl_3$ to obtain a shiny white crystalline solid. The solid was dried in a reduced pressure in a desiccator to afford 2.14 g (40.3 %) of **ABH-18**.

^{1}H NMR (400 MHz, $CDCl_3$, r.t.): δ 0.91 (t, J = 7.1 Hz, 3H), 1.27-1.51 (m, 30H), 1.81

(quin, J = 7.1 Hz, 2H), 4.02 (t, J = 6.6 Hz, 2H), 6.93 (d, J = 8.8 Hz, 2H), 8.06 (d, J = 9.3 Hz, 2H).

(d) 1-(4′-*n*-decyloxybenzoyl)-2-(4′-*n*-octadecyloxybenzoyl)hydrazine (BABH-10-18)

A mixture of compound **ABA-10** (2.21 g, 7.94 mmol) and an excess amount of thionyl chloride (25 mL, 42.00 g, 353 mmol) was stirred under reflux for 3 h. After cooling to room temperature, the remaining thionyl chloride was removed thoroughly under vacuum. To this solution was added dropwise a solution of the **ABH-18** (2.14 mmol, 5.29 mmol) dissolved in a dry THF. After finishing the addition, the solution was further stirred for 2 h. The resulting whipped solution was filtered and the residue was fully washed with water. The crude product was recrystallized from THF and then from $CHCl_3$ to obtain a white crystalline solid (0.76 g, 21.6%).

^{1}H NMR (400 MHz, $CDCl_3$, r.t.): δ 0.88 (dt, J = 1.94, 4.88 Hz, 6H), 1.26-1.49 (m, 44H), 1.80 (quin, J = 7.1 Hz, 4H), 3.99 (t, J = 6.6 Hz, 4H), 6.91 (d, J = 8.8 Hz, 4H), 7.82 (d, J = 8.8 Hz, 4H), 9.35 (s, 2H); Elemental Anal. Calcd for $C_{42}H_{68}N_2O_4$(%): C, 75.86; H, 10.31; N, 4.21; Found: C, 75.82; H, 10.15; N 4.22.

1.2 Preparation of equimolar mixtures of BABH-10 and -18, and BABH-8 and -20.

Equimolar amounts of two BABH-*n* samples were dissolved in THF. After that, the solution was heated to 100 °C to remove the solvent and further mixed at 160 °C in the molten state. Finally, the mixture was allowed to cool down to room temperature.

2. Measurements

^{1}H NMR (400 MHz) spectra were recorded on a JEOL JNM-α400 spectrometer and tetramethylsilane (δ = 0.00) was used as the internal standard. $CDCl_3$ or $(CD_3)_2SO$ was used as solvent. Microanalyses were carried out at Laboratory of Organic Elemental Microanalysis, Kyoto University, and performed using a J-Science Labo micro corder JM10, at Division Instrumental Analysis, Life Science Research Center, Gifu University.

Phase transitions were determined by using a Seiko Denshi DSC-200 interfaced to a TA data station (SSC 5000 system) and a SII Nanotechnologies DSC7020. The measurements were performed under a dry N_2 flow of *c*. 40 mL min^{-1} and the scanning rate was 5 K min^{-1}.

The texture of each mesophase was observed usually under crossed polarizers using polarizing optical microscopes (POM; a Nikon Optiphot-pol XTP-11 and an Olympus BX53P) equipped with a Mettler FP82HT hotstage and a Mettler FP90 controller. The scanning rate was 5 or 1 K min^{-1}. For the observation of a conglomerate of chiral domains, the sample was cooled to an objective temperature after holding it at a temperature in the

isotropic liquid state. The cooling rate was 10 K min^{-1} and the sample thickness was 44 μm using a PET film. The brightness of the two kinds of domains were inverted when the position of the analyzer was changed from +10° to −10° out of the precise 90° position with respect to the polarizer.

X-ray diffraction (XRD) patterns at elevated temperatures were obtained for powder samples using a Rigaku NANO-Viewer IP system. CuKα radiation was used at 45 kV and 60 mA. The scattered X-rays were recorded on a two-dimensional imaging plate (IP). The intensities were radially integrated and averaged, and redistributed when converting the pixel number into the corresponding scattering vector q ($q = (4\pi/\lambda)\sin\theta$, with λ being the X-rays wavelength (= 0.15418 nm) and 2θ the scattering angle) to produce a circularly averaged pattern. In some cases, to confirm the phase behaviors in detail, time-resolved XRD measurements were performed using synchrotron radiation at the Photon Factory (PF) in the High-Energy Accelerator Research Organization (KEK).

3. Some supplementary data on phase behaviors of the samples

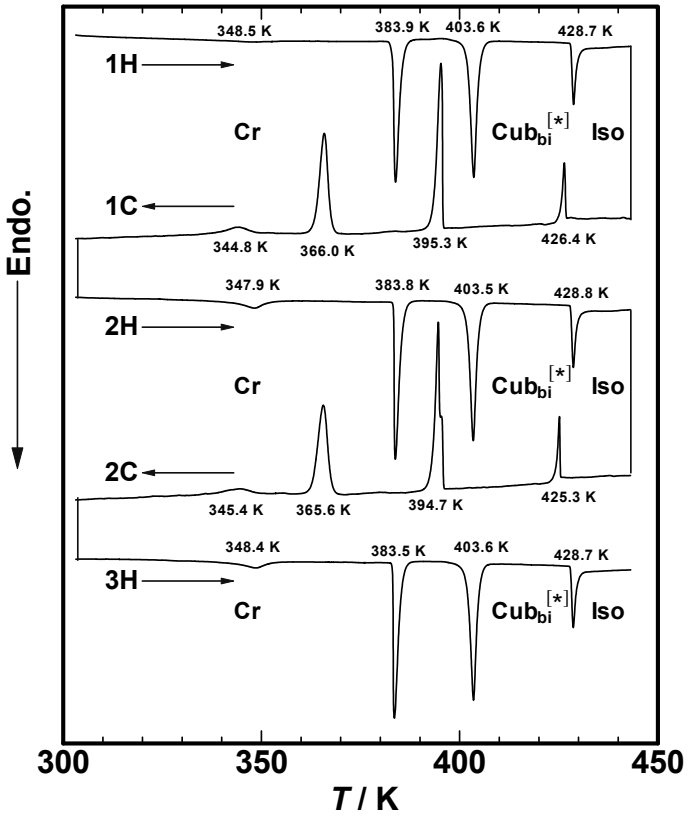

Fig. S1. DSC thermogram for equimolar mixture of **BABH-10** and **-18** (5 K min^{-1}).

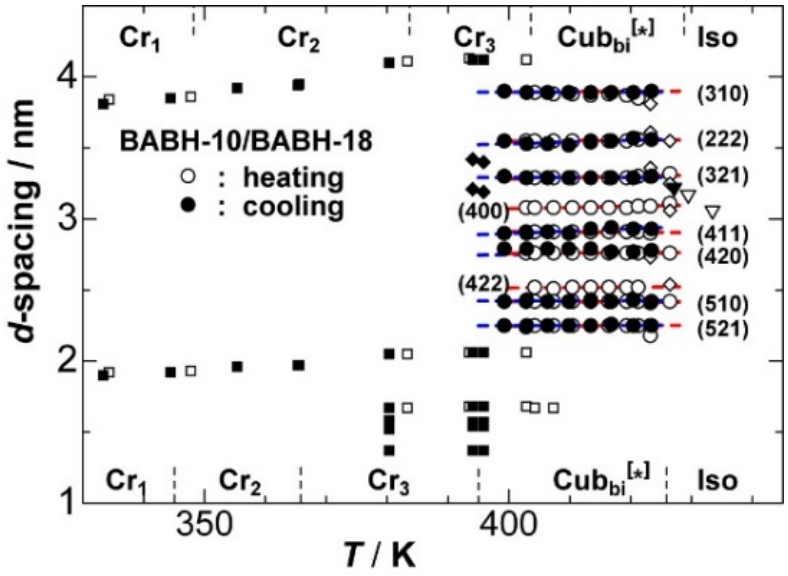

Fig. S2. Plots of *d*-spacings versus temperature both on heating (empty symbols) and on cooling (filled symbols) for equimolar mixture of **BABH-10** and **-18**; open diamonds indicate un-assignable reflections because of the instability of the phase in the vicinity of the isotropic liquid (Iso) phase.

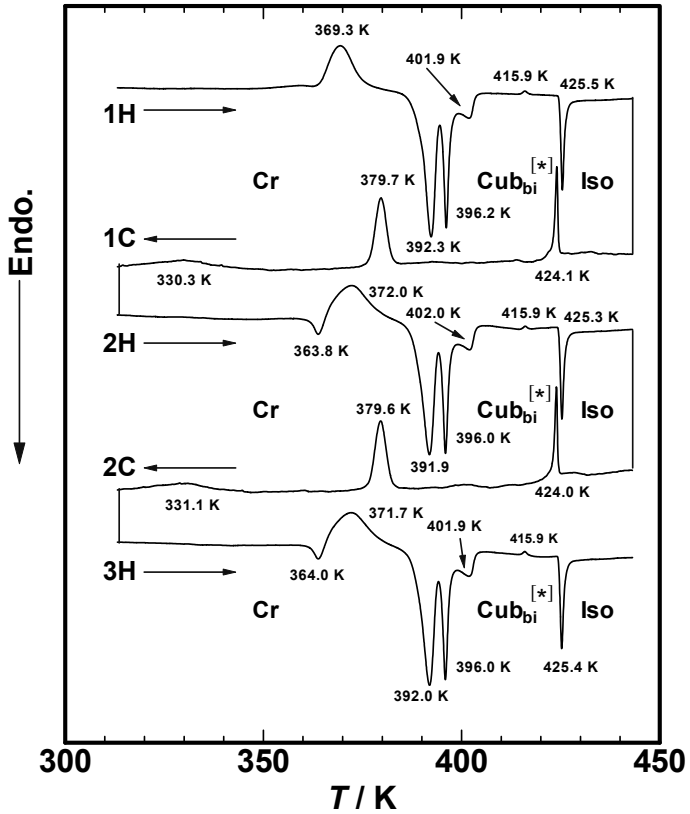

Fig. S3. DSC thermogram for equimolar mixture of **BABH-8** and **-20** (5 K min^{-1}).

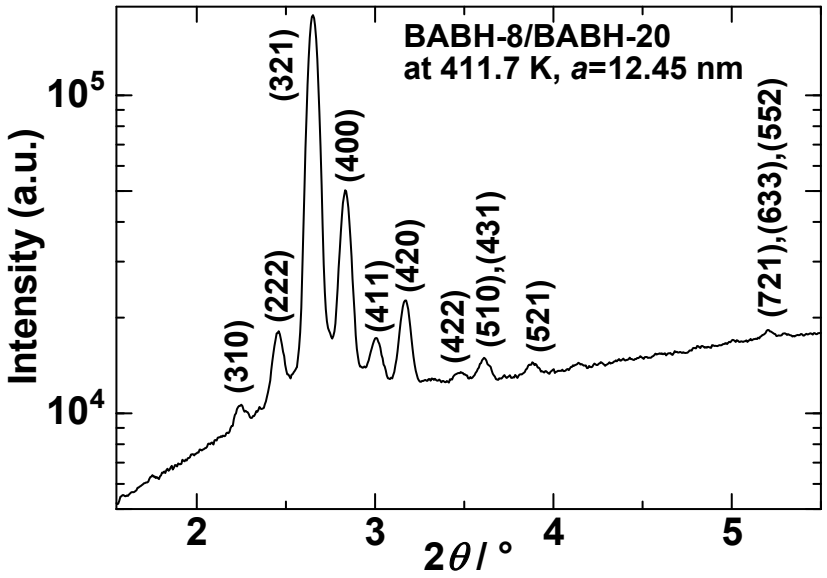

Fig. S4. XRD pattern for equimolar mixture of **BABH-8** and **-20** recorded at 411.7 K on heating.

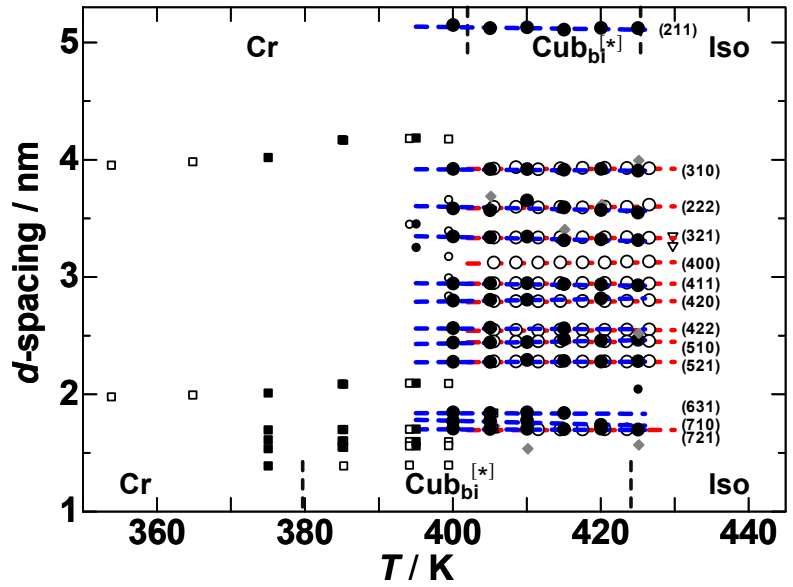

Fig. S5. Plots of *d*-spacings versus temperature both on heating (empty symbols) and on cooling (filled symbols) for equimolar mixture of **BABH-8** and **-18**. Gray square points obtained on cooling were not reasonably assigned to any cubic reflections; this is mainly due to the orientation of relatively larger domains which causes the uncertainty of the direct beam position.

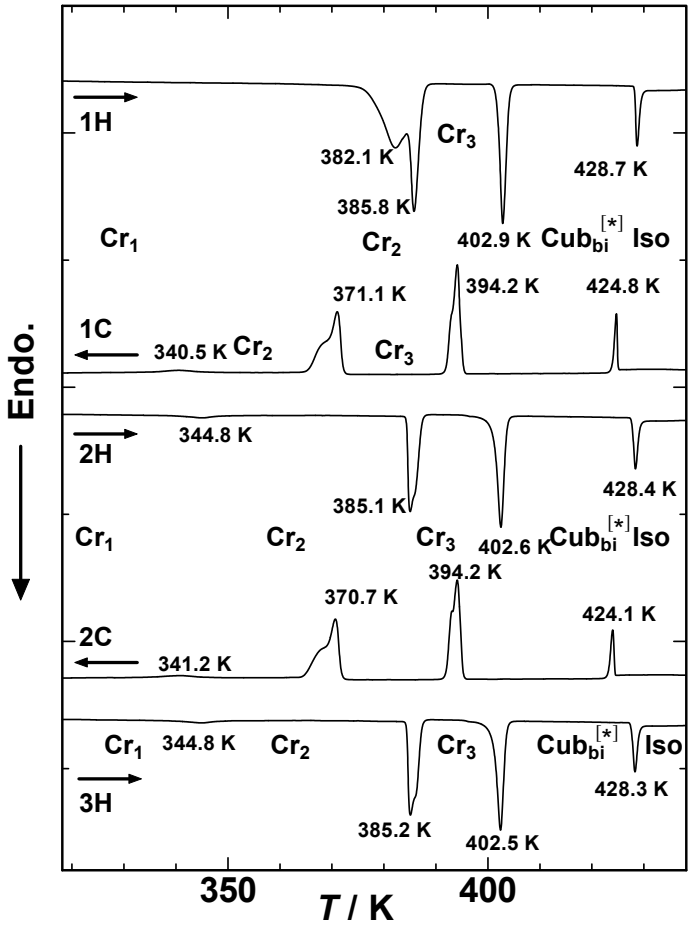

Fig. S6. DSC thermogram for **BABH-10-18** (5 K min^{-1}).

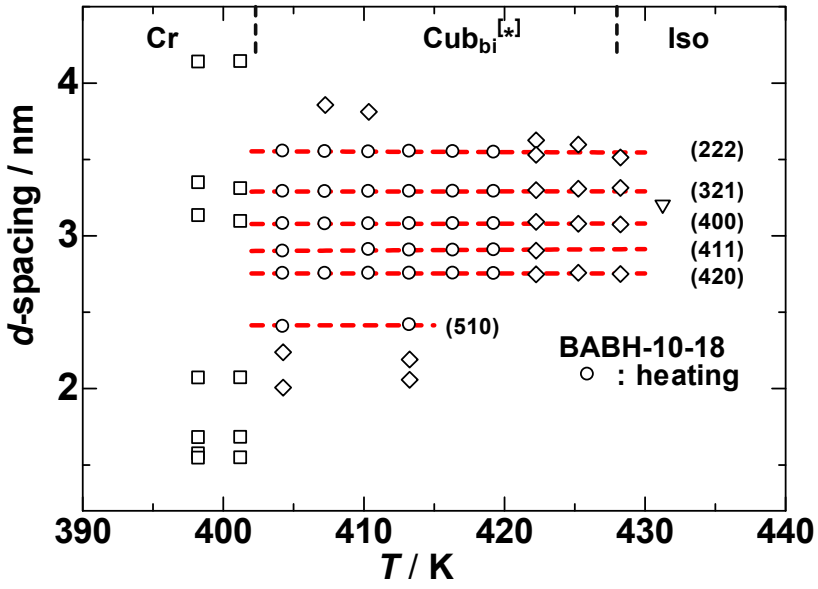

Fig. S7. Plot of *d*-spacings versus temperature on heating for **BABH-10-18**. Square symbols were not reasonably assigned to cubic reflections because of their peak splitting and/or irregular peak shape.

4. Reconstruction of electron density maps

For the evaluation of the peak intensities, the absence of preferred orientation was ascertained. All the detected peaks were reasonably approximated to a Gaussian line shape and so that the peak area intensities and their errors were estimated through curve fitting using a graph software Sma4Win ver. 1.54 (produced and distributed by T. Suzuki). The Lorentz correction on them yielded the final intensities. Table S1 summarizes the experimental magnitude of structure factors ($|F_{obs}|$) and errors ($\sigma(F_{obs})$) estimated together with the estimated ones (F_{calc}) through maximum entropy method (MEM) analyses described below.

The reconstruction of electron density maps was performed using the structure factors $|F_{obs}|$. The calculation was made using a laboratory-made code and the space of the unit cell was divided into 128×128×128 pixels. The Landau theory of freezing for the *Im*3*m* phase formation requires the same signs of the structure factors for the two strongest reflections {321} and {400}.[S3] In our MEM analyses, the signs were assumed to be both – because the fraction of region having higher electron density than the average should be less than the half, while those of the others are automatically determined during the MEM optimization process. The detailed procedure was already published.[S4]

Table S1. SAXS data used for the MEM analyses (Insets of Fig. 1) of the chiral Cub_{bi} phase of three samples.

	BABH-14 at 421.7 K			mix. of **BABH-10** and **-18** at 421.0 K			**BABH-10-18** at 419.3 K		
(*hkl*)	$\|F_{obs}\|$	F_{calc}	$\sigma(F_{obs})$	$\|F_{obs}\|$	F_{calc}	$\sigma(F_{obs})$	$\|F_{obs}\|$	F_{calc}	$\sigma(F_{obs})$
(211)	0.047	0.051	0.013	-	-	-	-	-	-
(310)	0.119	0.106	0.014	0.103	0.101	0.011	0.077	0.077	0.004
(222)	0.284	-0.268	0.012	0.429	0.292	0.024	0.329	-0.239	0.021
(321)	0.714	-0.714	0.003	0.714	-0.722	0.016	0.688	-0.688	0.003
(400)	1.000	-1.000	0.008	1.000	-1.000	0.034	1.000	-1.000	0.010
(411)	0.158	0.155	0.010	0.284	0.258	0.021	0.195	0.194	0.011
(420)	0.243	0.243	0.006	0.305	-0.309	0.006	0.251	0.251	0.003
(332)	0.078	0.056	0.023	0.142	-0.129	0.017	0.031	0.030	0.019
(422)	0.110	0.039	0.024	0.119	0.120	0.007	0.064	0.063	0.007
(431)	0.083	0.082	0.008	0.092	-0.093	0.003	0.082	0.082	0.006
(521)	0.065	0.060	0.012	0.068	-0.069	0.004	0.064	0.064	0.005
(440)	0.084	0.114	0.035	-	-	-	-	-	-
(541)	0.049	0.048	0.010	0.034	0.033	0.008	-	-	-
(631)	-	-	-	0.040	0.042	0.009	-	-	-
(444)	0.157	0.115	0.030	-	-	-	-	-	-
(640)	0.092	0.056	0.021	-	-	-	0.131	0.063	0.029
(642)	0.051	0.048	0.011	0.044	-0.045	0.005	0.063	0.056	0.015

$|F_{obs}|$ and F_{calc}, experimental and calculated F values, normalized to $|F(400)|$; $\sigma(F_{obs})$, error; "-" indicates nonobserved reflection within the experimental 2θ range.

4.1 Electron density map for Cub_{bi} [*] phase of BABH-14

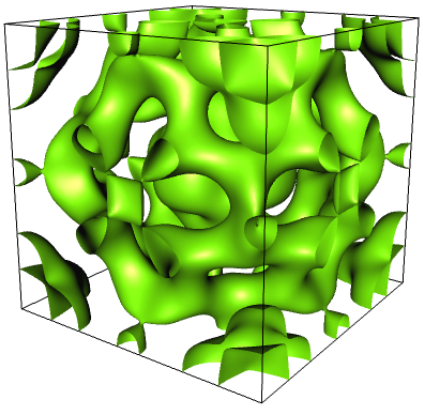

Equal-density plane

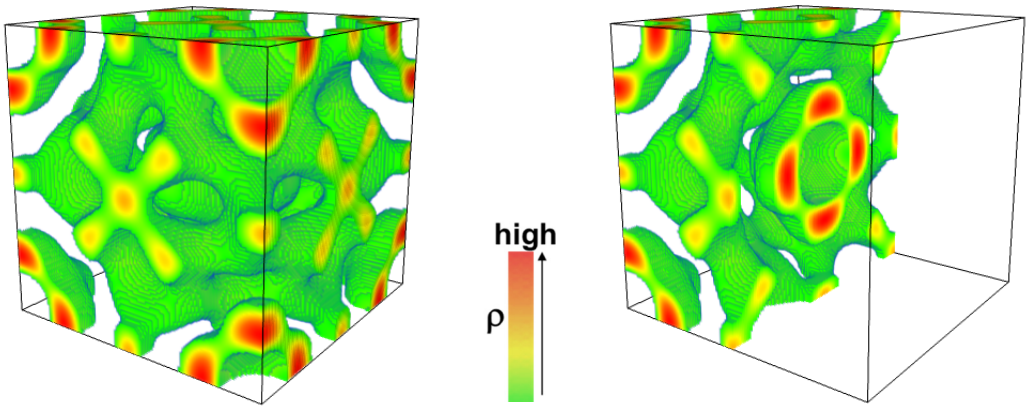

Density map

Fig. S8. Electron density map reconstructed for the Cub_{bi}[*] phase of **BABH-14** at 421.7 K using MEM optimization method. The region with a smaller density than the average is shown transparent.

4.2 Electron density map for Cub_{bi} [*] phase of a 1:1 mixture of BABH-10 and -18

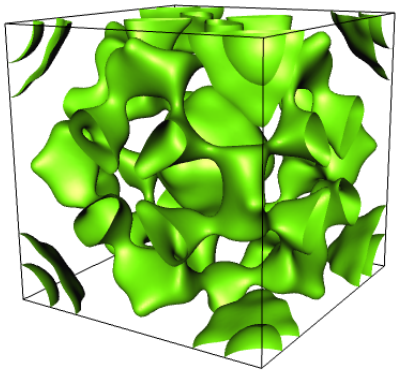

Equal-density plane

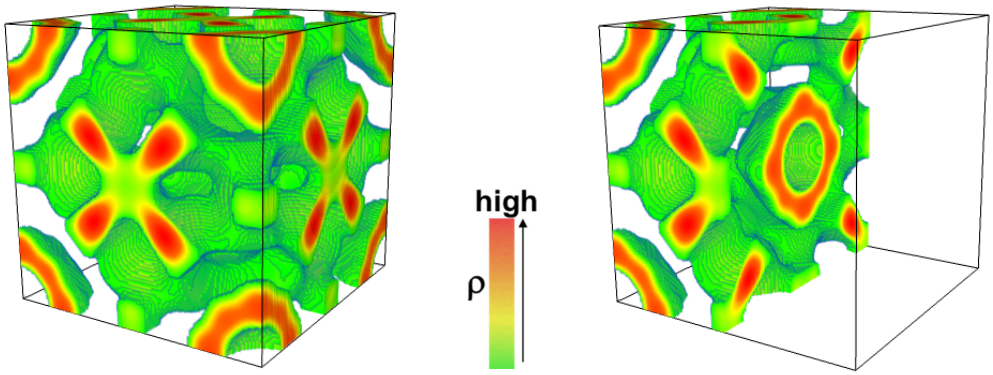

Density map

Fig. S9. Electron density map reconstructed for the Cub_{bi}[*] phase of equimolar mixture of **BABH-10** and **-18** at 421.0 K.

4.3 Electron density map for Cub_{bi} [*] phase of BABH-10-18

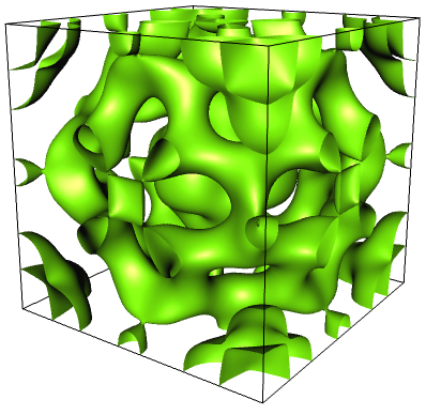

Equal-density plane

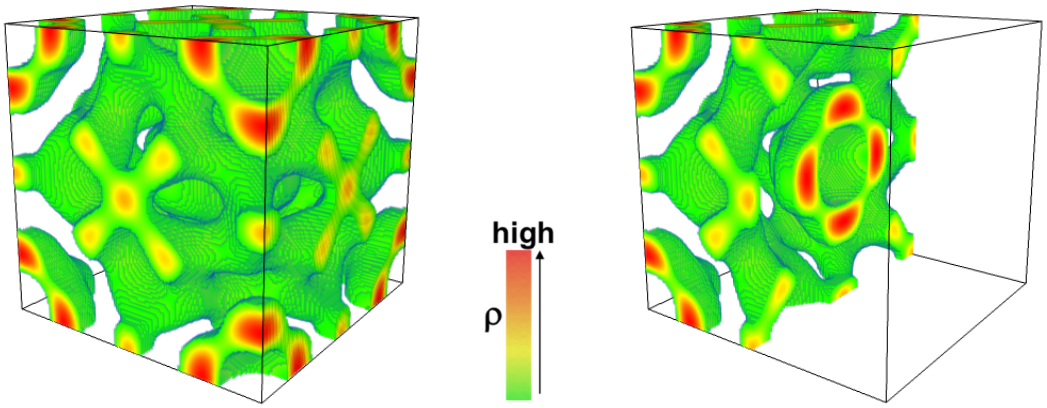

Density map

Fig. S10. Electron density map reconstructed for the Cub_{bi}[*] phase of **BABH-10-18** at 419.3 K using MEM optimization method.

4.4 Short note on *Ia3d*-gyroid phase structure

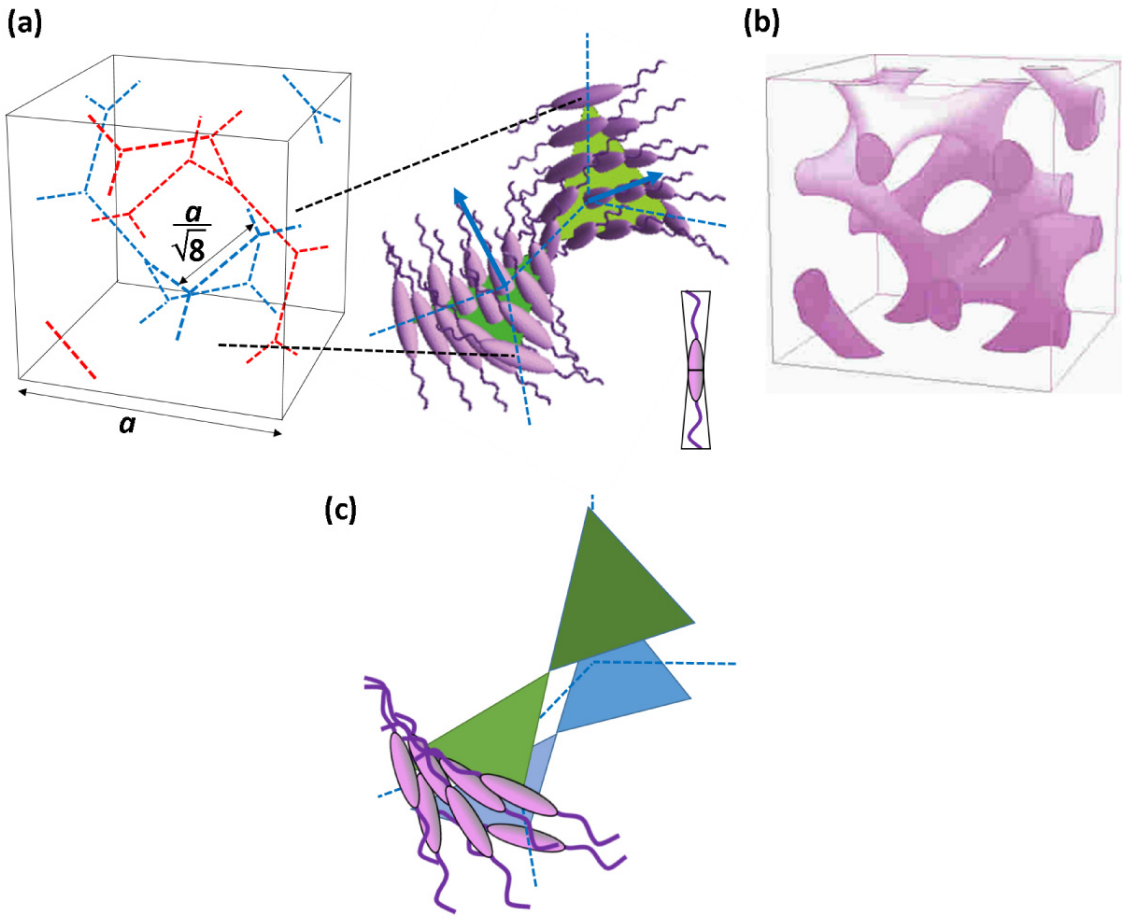

Fig. S11. Schematic representation of *Ia3d* gyroid phase structure: (a) Two networks (red and blue broken lines) embedded in the unit cell (*a*: cell dimension). Each network is constructed by connected segments with a length of $a/\sqrt{8}$ and three segments meet at the junctions; each three-fold junction is in a triangular plane (green-colored), and two neighboring planes (blue bold arrows in the figure are their normal vectors) are twisted with each other, with a dihedral angle of 70.5°. This is a "single-layered core" state for short-chain BABH molecules such as **BABH-10**.[S5] The side-by-side arrangement of the constituent molecules with just like a two-megaphone-connected shape ("tapered shape") causes a molecular twist along the network,[S2,S5] although opposite handedness of the two networks cancels the chirality in the *Ia3d*-Cub$_{bi}$ phase; (b) Three-dimensional network of a finite size composed of aggregated cores (violet-colored); and (c) "Doubled-layered core" state for long-chain BABH molecules such as **BABH-18**. The layer of the molecular cores is split into two (green and blue triangular planes), at both sides of the network lines (blue broken lines), which was elucidated by our previous investigation.[S5]

References in this SI

[S1] H. Schubert, J. Hauschild, D. Demus and S. Hoffmann, *Z. Chem.,* 1978, **18**, 256–256.

[S2] S. Kutsumizu, H. Mori, M. Fukatami, S. Naito, K. Sakajiri and K. Saito, *Chem. Mater.*, 2008, **20**, 3675–3687.

[S3] K. Saito, Y. Yamamura and S. Kutsumizu, *J. Phys. Soc. Jpn.*, 2008, **77**, 093601.

[S4] K. Ozawa, Y. Yamamura, S. Yasuzuka, H. Mori, S. Kutsumizu and K. Saito, *J. Phys. Chem. B*, 2008, **112,** 12179–12181.

[S5] Y. Nakazawa, Y. Yamamura, S. Kutsumizu and K. Saito, *J. Phys. Soc. Jpn.*, 2012, **81**, 094601.